Uncertainty in least-squares fits to the thermal noise spectra of nanomechanical resonators with applications to the atomic force microscope

John E. Sader,[1,a)] Morteza Yousefi,[2] and James R. Friend[2,3]
[1]*Department of Mathematics and Statistics, The University of Melbourne, Victoria 3010, Australia*
[2]*MicroNanophysics Research Laboratory, RMIT University, Melbourne, Victoria 3001, Australia*
[3]*Melbourne Centre for Nanofabrication, Clayton, Victoria 3800, Australia*

(Received 31 July 2013; accepted 20 January 2014; published online 14 February 2014)

Thermal noise spectra of nanomechanical resonators are used widely to characterize their physical properties. These spectra typically exhibit a Lorentzian response, with additional white noise due to extraneous processes. Least-squares fits of these measurements enable extraction of key parameters of the resonator, including its resonant frequency, quality factor, and stiffness. Here, we present general formulas for the uncertainties in these fit parameters due to sampling noise inherent in all thermal noise spectra. Good agreement with Monte Carlo simulation of synthetic data and measurements of an Atomic Force Microscope (AFM) cantilever is demonstrated. These formulas enable robust interpretation of thermal noise spectra measurements commonly performed in the AFM and adaptive control of fitting procedures with specified tolerances. © *2014 AIP Publishing LLC*. [http://dx.doi.org/10.1063/1.4864086]

I. INTRODUCTION

The mechanical and energetic properties of nanomechanical resonators are commonly measured from their thermal noise spectra.[1–13] This provides a sensitive and often non-invasive means of characterizing small-scale devices. The Lorentzian distribution normally describes with good accuracy the functional form of the thermal noise power spectrum in the neighborhood of a single mechanical resonance, especially for resonators possessing high quality factors.[14] Extraneous and independent noise processes, such as those in the detector, provide additional spectral contributions that can be collectively modeled as a white noise process in the vicinity of resonance;[15] this is used widely in Atomic Force Microscope (AFM) measurements. Combination of these noise processes leads to the following model:

$$S(f|A_{\text{white}}, B, f_R, Q) = A_{\text{white}} + \frac{B}{4Q^2\left(\frac{f}{f_R} - 1\right)^2 + 1}, \tag{1}$$

which is frequently applied to interpret measurements of the thermal noise power spectrum; f is the frequency variable. The model contains four fit parameters: white noise amplitude, A_{white}, amplitude at resonance, B, resonant frequency, f_R, and quality factor, Q. These parameters are determined using a least-squares fit to experimental data.

In practice, the thermal noise spectrum is typically measured using (finite) time series samples of Brownian motion of the resonator, which are subsequently windowed, Fourier transformed, and averaged together.[16] Formally, the thermal noise spectrum is determined from the ensemble average over all realizations of the noise process. Since only a finite number of averages can be performed in practice, all measurements of the thermal noise spectrum intrinsically contain uncertainty, i.e., sampling noise.[16] The standard deviation of this sampling noise is directly proportional to the magnitude of the thermal noise power spectrum, i.e., the power spectral density (PSD) of the noise process, at any given frequency; the sampling noise is multiplicative.[16,17] This sampling noise affects the precision of model fits to the measured thermal noise spectrum, leading to unavoidable uncertainty in parameter estimation from a least-squares analysis. An example using synthetic data is given in Fig. 1, where significant deviations between the true and fit parameters are observed. Quantifying this uncertainty is vital for a proper analysis of measurements and rigorous interpretation of their underlying physics.

Recently, we presented a general theory[17] enabling calculation of the uncertainty in parameters extracted from a least-squares fit to measurements containing multiplicative noise. This analysis is directly relevant to the interpretation of measurements of the thermal noise spectrum; see above. Explicit formulas for the standard deviation in the fit parameters were derived when the model used is purely Lorentzian, i.e., no white noise is present. These formulas were found to agree well with (i) Monte Carlo simulations of synthetic data, and (ii) experimental measurements on an AFM cantilever of low stiffness, and hence small/negligible background (white) noise. However, there exist many practical situations where the background noise is not small, and indeed dominates the response. This is especially the case for devices of high stiffness, whose thermomechanical motion is comparable to the detection sensitivity limit.

The purpose of this article is to report analytical formulas for the uncertainty in fit parameters when the thermal noise spectrum and model function contain arbitrary levels of background (white) noise. This calculation is performed using the general theory presented in our previous study.[17] White noise

a)Email: jsader@unimelb.edu.au

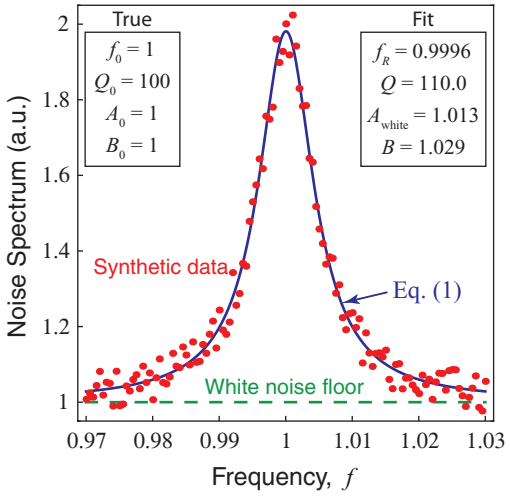

FIG. 1. Sample synthetic noise spectrum data [red dots] and fit to Eq. (1) [solid curve]. True spectrum parameters shown in left inset, and defined in Eq. (2). Extracted fit parameters from a least-squares analysis given in right inset. White noise floor [dashed line]. Simulations performed as in Ref. 17, and described below.

is found to strongly enhance uncertainty in the resulting fit parameters. The reported formulas are expected to be of value to users and designers of AFM cantilevers, as we shall discuss.

The effect of using different fit models that exactly describe the same measurement is also studied. It is found that uncertainty in the resulting fit parameters can be model dependent. This motivates further studies to optimize models for maximum fit precision.

II. FORMULAS FOR UNCERTAINTY IN FIT PARAMETERS

In the ideal limit of no sampling noise, a least-squares fit to Eq. (1) would recover the true (exact) parameters of the resonator

$$A_{\text{white}} = A_0, \quad B = B_0, \quad f_R = f_0, \quad Q = Q_0, \tag{2}$$

where the subscript "0" indicates a true value. Throughout, we study a least-squares fit performed over a finite frequency interval: $f \in [f_{\min}, f_{\max}]$, with $f_{\min} = f_0(1 - \beta/Q_0)$ and $f_{\max} = f_0(1 + \beta/Q_0)$. The constant β defines the span in frequency of the fit window, normalized by the spectral width of the Lorentzian peak, i.e., $2f_0/Q_0$.

Any sampling noise in measurements will lead to uncertainty, and inevitably, deviations in the fit parameters from their true values in Eq. (2), e.g., see Fig. 1. The general theory in Ref. 17 enables direct calculation of the standard deviations (or variances) in these fit parameters due to the presence of sampling noise, which is taken to be small. Assuming the fit window is much larger than the spectral width of the Lorentzian, i.e., $\beta \gg 1$, we obtain the required formulas

$$\frac{\text{SD}[A_{\text{white}}]}{A_0} = \alpha\sqrt{\frac{\pi}{\beta} + \frac{\pi^2(16\lambda^2 + 4\lambda + 1)}{16\lambda^2\beta^2} + O\left(\frac{1}{\beta^3}\right)}, \tag{3a}$$

$$\frac{\text{SD}[B]}{B_0} = \alpha\sqrt{13 + 28\lambda + 16\lambda^2 - \frac{4(1+2\lambda)}{\beta^2} + O\left(\frac{1}{\beta^3}\right)}, \tag{3b}$$

$$\frac{\text{SD}[f_R]}{f_0} = \frac{\alpha}{2Q_0}\sqrt{7 + 20\lambda + 16\lambda^2 + \frac{2(7 + 20\lambda + 8\lambda^2)}{5\pi\beta^5} + O\left(\frac{1}{\beta^6}\right)}, \tag{3c}$$

$$\frac{\text{SD}[Q]}{Q_0} = 2\alpha\sqrt{(3+8\lambda+8\lambda^2)\left(1+\frac{\pi}{2\beta}\right)+\frac{7+20\lambda+16\lambda^2}{16Q_0^2}+O\left(\frac{1}{\beta^2}\right)}, \tag{3d}$$

where α is defined

$$\alpha \equiv \sqrt{\frac{Q_0}{2\pi f_0 T}}, \tag{4}$$

where T is the total measurement time, and $\lambda \equiv A_0/B_0$ is the ratio of the true white noise amplitude to the true resonance amplitude. Since β specifies the span of the fit window $f \in [f_{\min}, f_{\max}]$, and Eqs. (3a)–(3d) are derived for $\beta \gg 1$, these equations implicitly assume $Q_0 \gg 1$; exact formulas for arbitrary β and Q_0 are given in the supplementary material.[18] SD[X] denotes the standard deviation of any variable X. Note that the standard deviations of all fit parameters are independent of the number of averages used to determine the thermal noise spectrum; they depend only on the total measurement time, as discussed in Ref. 17.

The area under the Lorentzian term in Eq. (1), denoted Π, is also frequently required in practice. Its standard deviation is specified by

$$\frac{\text{SD}[\Pi]}{\Pi_0} = \alpha\sqrt{3 + 12\lambda + 16\lambda^2 + \frac{2\pi(1+4\lambda+8\lambda^2)}{\beta} + O\left(\frac{1}{\beta^2}\right)}. \tag{5}$$

The formulas in Eqs. (3b)–(3d) and (5) show that as the white noise level rises, the uncertainty in all other fit parameters increases. This is not surprising given that the relative contribution from the Lorentzian function diminishes with increasing background (white) noise. In the limit of very large white noise, $\lambda \gg 1$, uncertainty in the white noise amplitude, Eq. (3a), plateaus to a constant value. Increasing the fit range parameter β reduces this uncertainty, which is also as expected since more data are used in the least-squares analysis. Equations (3a), (3c), (3d), and (5) show that increasing β decreases the fit uncertainties in A_{white}, f_R, Q, and Π. To minimize these uncertainties in practice, β should be chosen as large as possible while ensuring that the measured PSD data match the form of Eq. (1). The formulas in Eqs. (3a)–(3d) and (5) are the results we seek and enable the uncertainty in fit parameters to be determined in practice.

III. VALIDATION OF FORMULAS

We now assess the validity and accuracy of these formulas by comparison to (i) Monte Carlo simulations of synthetic noisy data, for fixed λ and varying β, and (ii) measurements on an AFM cantilever, as a function of λ at fixed β.

A. Monte Carlo simulations of synthetic data

Details of the Monte Carlo simulations are identical to those in Ref. 17, except a white noise term is now included. Specifically, synthetic data are derived by taking a reference Lorentzian plus white noise function (with specified $f_0 = 1$, $Q_0 = 100$, $A_0 = 1$, $B_0 = 1$), discretizing the function in f (by $\delta f = f_0/(10\,Q_0)$), multiplying each discrete value by a uniformly distributed random variable, ϵz_k, where $z_k \in [-1, 1]$ and $\epsilon = 0.001$ is a fixed small constant, and adding the result to the reference. This corresponds to setting $T = 1/[\delta f(\mathrm{SD}[\epsilon \delta z_k])^2]$ in Eqs. (3a)–(3d) and (5); see Ref. 17. A total of 100 000 realizations of this noisy data are simulated, which are then individually fit to Eq. (1) using a least-squares analysis. This is performed for a range of fit window sizes, $\beta \in [2, 10]$, to ensure a substantial portion of the resonance peak is fitted and the large-β regime is probed. The standard deviations of all fit parameters, f_R, Q, B, and A_{white}, are then computed and compared to the predictions of Eqs. (3a)–(3d) and (5).

Figure 2 shows that these formulas accurately predict the synthetic data, especially for large fit window size, β. This is as expected, since Eqs. (3a)–(3d) and (5) are asymptotic formulas derived in the limit of large β. At smaller values of β, discrepancies occur in formulas for the quality factor, Q, and area under the Lorentzian, Π. Inclusion of the next higher-order term in these asymptotic expansions, at $O(1/\beta^2)$, improves matters significantly; see dashed lines in Fig. 2. The correction of $O(1/\beta^2)$ for Q in Eq. (3d) is

$$[(7\pi^2 - 44) + 4(5\pi^2 - 32)\lambda + 16(\pi^2 - 6)\lambda^2]\frac{1}{\beta^2},$$

whereas the result for Π in Eq. (5) is

$$[3(\pi^2 - 4) + 4(3\pi^2 - 14)\lambda + 16(\pi^2 - 4)\lambda^2]\frac{1}{\beta^2}.$$

These higher order corrections ensure that all formulas are specified to $O(1/\beta^2)$; these add a significant level of complexity to the formulas, and are included here for completeness.

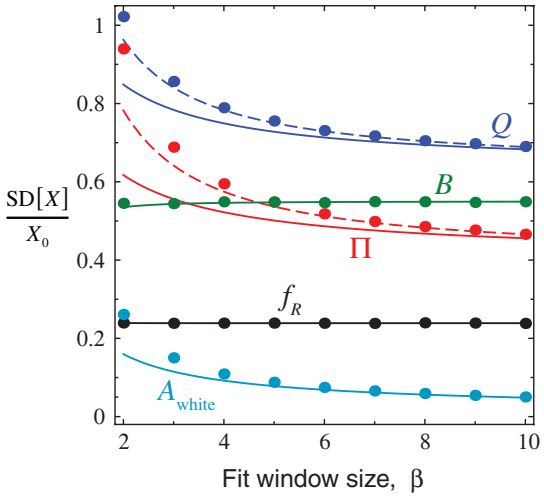

FIG. 2. Comparison of normalized relative standard deviations, $\mathrm{SD}[X]/X_0$, of synthetic data [dots] and Eqs. (3a)–(3d) and (5) [lines]. Variable X represents a specific parameter (f_R, Q, A_{white}, B, Π), with results for f_R multiplied by Q_0, i.e., $Q_0\mathrm{SD}[f_R]/f_0$ is plotted. Dashed lines for $\mathrm{SD}[Q]/Q_0$ and $\mathrm{SD}[\Pi]/\Pi_0$ include an additional term of $O(1/\beta^2)$. Data and formulas normalized by $\epsilon = 0.001$.

B. Measurements of an AFM cantilever

The presented formulas are now compared to experimental measurements of the Brownian fluctuations of an AFM cantilever. The thermal noise spectra of this cantilever are measured at a range of discrete positions along its length. Because the local stiffness varies strongly with position, varying the measurement position enables adjustment of the resonance amplitude, B, relative to the (position independent) background white noise amplitude, A_{white}. These measurements are performed on the fundamental mode of a Bruker MLCT (Lever B) cantilever in air using a laser Doppler vibrometer (LDV); MSA-500 Micro System Analyzer, Polytec (Waldbronn, Germany), VD-09 2.5 MHz Digital Velocity Decoder, measurement range of 100 mm/s/V. The cantilever has a nominal spring constant of 0.02 N/m (at its imaging tip position), resonant frequency of $f_0 = 13.4$ kHz, and quality factor of $Q_0 = 21$.

At each position on the cantilever, the following measurement and analysis protocol is performed. Time series of total duration 1000 s is measured at a sampling frequency of 51.2 kHz. This time series is divided into $T = 1$ s intervals, each of which is subdivided into 50 subintervals of duration 20 ms. Periodograms of these 20 ms subdivisions are computed and averaged together. This gives 1000 estimates of the PSD at each measurement position, which are individually fitted to Eq. (1) using a frequency range 7.4 kHz $\leq f \leq$ 19.2 kHz; see Fig. 3. Histograms of the fit parameters are

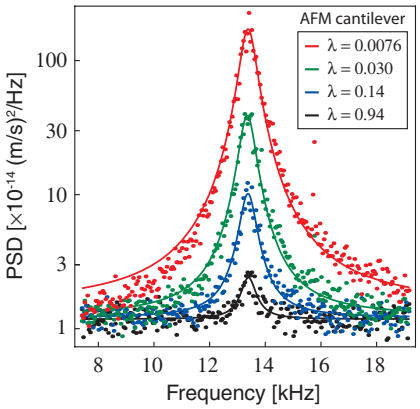

FIG. 3. PSD measurements at 4 different positions on an AFM cantilever, determined using time series of duration $T = 1$ s that is subdivided into fifty 20 ms intervals. Measurement data [dots]; fits to Eq. (1) [lines]. Resonance peaks of higher magnitude correspond to measurements closer to the cantilever free end, in accord with the equipartition theorem; a white noise floor $\approx 1.2 \times 10^{-14}$ (m/s)^2/Hz is present in all measurements.

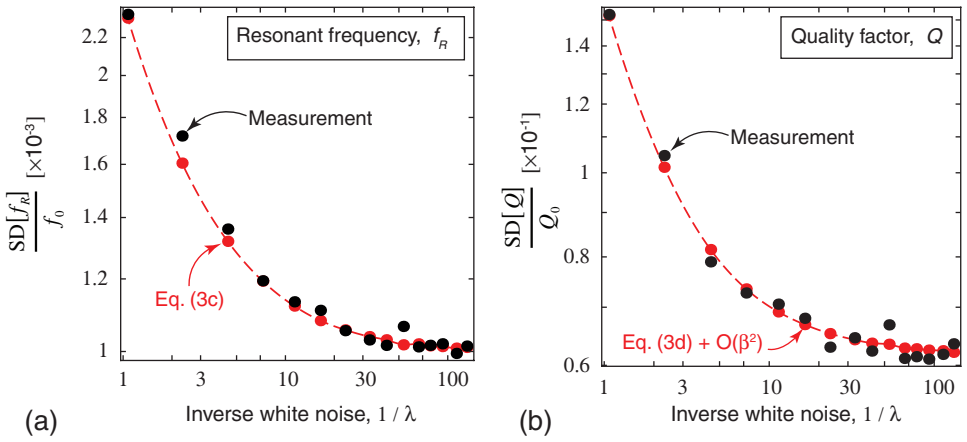

FIG. 4. Comparison of measurement [black] and theory [red] for the relative standard deviation in the fitted resonant frequency, f_R, and quality factor, Q. Results given as a function of the relative magnitude of white noise, λ. Formula for the quality factor includes the $O(\beta^2)$ correction.

then generated (not shown), from which their mean and standard deviation are determined. Measurements over a series of positions on the cantilever yield results in the range $0.008 \leq \lambda \leq 0.94$, enabling robust assessment of the presented formulas. Measured spectra for the $T = 1$ s time interval at select positions on the cantilever are shown in Fig. 3, together with fits to Eq. (1); larger λ corresponds to smaller distance of the measurement position from the clamped end of the cantilever.

Measured standard deviations in the fitted resonant frequency and quality factor are given in Fig. 4, together with the predictions from Eqs. (3c) and (3d). Equations (3c) and (3d) require specification of the relative amplitude λ, which is obtained from the mean of the fitted white noise amplitudes, A_0, and resonance amplitudes, B_0. Note the excellent agreement between theory and measurement in all cases; the relative standard deviation in the residual between theory and measurement is less than 2.5%, for both the resonant frequency and quality factor. As predicted above, uncertainty in the fit parameters increases with white noise amplitude. These results, together with those in Fig. 2 for the synthetic numerical data, demonstrate the validity of the presented formulas.

Thermal drift is unavoidable in measurements and results in a slight defocusing of the optics and movement of the laser position on the cantilever, over the measurement time of 1000 s. Consequently, the white noise and resonance peak amplitudes are slightly time dependent, which enhances their measured (small) standard deviations; measured standard deviations of these fitted amplitudes, i.e., A_{white}, B, and Π, are therefore not reported. For this reason, formulas for the standard deviations of these parameters must be considered lower bounds in practice, as discussed in Ref. 17.

C. Effect of using different fit models

Finally, we examine the performance of these formulas in the ideal case where no white noise exists in the measurement and the response is purely Lorentzian. Strictly, the white noise term in Eq. (1) is not required in such a situation. It is therefore of interest to explore its effect on fit precision. Table I compares formulas for the standard deviations in the fit parameters for two model functions: (A) The previous model in Eq. (10) of Ref. 17 that does not contain a white noise term, and (B) the model in Eq. (1) that includes this term. These two models thus correspond to functions with 3 and 4 degrees of freedom, respectively, that exactly describe the measurement, i.e., the models are not biased.

In the limit of infinite fit window size, $\beta \to \infty$, the uncertainty formulas for both models coincide. Thus, there is no advantage to using one model over another here. The reason is that the white noise term cannot contribute to fits in this limit, because the measurement decays to zero as $f \to \infty$. Even so, we note that this formal limit cannot be realized in practice due to the presence of other device resonances and non-ideal response of the detector, e.g., finite frequency range as dictated by the Nyquist frequency.

Including a white noise term in the model enhances the dependence of fit parameter uncertainty on fit window size, β.

TABLE I. Formulas for the normalized standard deviations in fit parameters when no white noise is present in measurements, i.e., $\lambda = 0$. Two models: (A) Lorentzian function; (B) Lorentzian function + white noise term. Leading-order asymptotic expressions for large β and Q.

Model	$\left(\frac{\mathrm{SD}[B]}{\alpha B_0}\right)^2$	$\left(\frac{\mathrm{SD}[f_R]}{\alpha f_0}\right)^2$	$\left(\frac{\mathrm{SD}[Q]}{\alpha Q_0}\right)^2$	$\left(\frac{\mathrm{SD}[\Pi]}{\alpha \Pi_0}\right)^2$
(A) Lorentzian	$13 + \frac{6}{\pi\beta^3}$	$\frac{7}{4Q_0^2}\left(1 + \frac{2}{5\pi\beta^5}\right)$	$12 + \frac{7}{4Q_0^2} + \frac{26}{\pi\beta^3}$	$3 + \frac{16}{3\pi\beta^3}$
(B) Lorentzian + white noise	$13 - \frac{4}{\beta^2}$	$\frac{7}{4Q_0^2}\left(1 + \frac{2}{5\pi\beta^5}\right)$	$12 + \frac{7}{4Q_0^2} + \frac{6\pi}{\beta}$	$3 + \frac{2\pi}{\beta}$

Standard deviations in the quality factor, Q, and area under the Lorentzian, Π, now display a stronger $1/\beta$ dependence rather than $1/\beta^3$. The corresponding change in the resonance peak amplitude, B, is different, with a $1/\beta^2$ dependence instead of $1/\beta^3$. The observed reduction in the resonance peak amplitude uncertainty is likely due to the presence of two amplitude parameters in Eq. (1), A_{white} and B, that the least-squares analysis can use to describe this single physical feature of the thermal noise spectrum. Such enhancement in amplitude fit precision must come at the cost of reduced precision in fitting the true shape of the Lorentzian function; this is not possible at infinite window size, as discussed above. This feature is borne out in Table I, where uncertainties in the quality factor and area under the Lorentzian function are strongly enhanced. We note that the position of the resonance peak is unaffected by the presence of A_{white}, and uncertainty in the resonant frequency is identical for both models.

This discussion shows that use of different models, which exactly describe the same measurement, can lead to variable uncertainty in the resulting fit parameters. Judicious choice of fit model is therefore critical to achieving maximum precision; this can be performed using the general theory in Ref. 17.

IV. CONCLUSIONS

We have presented formulas for the standard deviation in fit parameters obtained from a least-squares analysis of the thermal noise spectrum of nanomechanical devices. These formulas assume a model that consists of a Lorentzian function and an arbitrary white noise term; such a response is widely observed in practice. The results presented in this study enable the optimization and design of measurements with specified tolerances. For example, the total measurement time required for a specified fit parameter tolerance can be determined directly. This enables adaptive control of fitting procedures and/or estimation of uncertainty post-measurement. These formulas will find particular application in the Atomic Force Microscope, where the thermal noise spectra of microcantilevers are commonly measured.

ACKNOWLEDGMENTS

The authors gratefully acknowledges the support of the Australian Research Council Grants Scheme.

[1] G. Binnig, C. F. Quate, and C. Gerber, Phys. Rev. Lett. **56**, 930 (1986).
[2] J. P. Cleveland, S. Manne, D. Bocek, and P. K. Hansma, Rev. Sci. Instrum. **64**, 403 (1993).
[3] J. L. Hutter and J. Bechhoefer, Rev. Sci. Instrum. **64**, 1868 (1993).
[4] J. E. Sader, J. W. M. Chon, and P. Mulvaney, Rev. Sci. Instrum. **70**, 3967 (1999).
[5] H. G. Craighead, Science **290**, 1532 (2000).
[6] N. V. Lavrik, M. J. Sepaniak, and P. G. Datskos, Rev. Sci. Instrum. **75**, 2229 (2004).
[7] K. L. Ekinci and M. L. Roukes, Rev. Sci. Instrum. **76**, 061101 (2005).
[8] T. Franosch, M. Grimm, M. Belushkin, F. M. Mor, G. Foffi, L. Forro, and S. Jeney, Nature (London) **478**, 85 (2011).
[9] A. Jannasch, M. Mahamdeh, and E. Schaeffer, Phys. Rev. Lett. **107**, 228301 (2011).
[10] J. te Riet, A. J. Katan, C. Rankl, S. W. Stahl, A. M. van Buul, I. Y. Phang, A. Gomez-Casado, P. Schön, J. W. Gerritsen, A. Cambi *et al.*, Ultramicroscopy **111**, 1659 (2011).
[11] J. E. Sader, J. A. Sanelli, B. D. Adamson, J. P. Monty, X. Wei, S. A. Crawford, J. R. Friend, I. Marusic, P. Mulvaney, and E. J. Bieske, Rev. Sci. Instrum. **83**, 103705 (2012).
[12] M. H. Matheny, L. G. Villanueva, R. B. Karabalin, J. E. Sader, and M. L. Roukes, Nano Lett. **13**, 1622 (2013).
[13] E. C. Bullard, J. Li, C. R. Lilley, P. Mulvaney, M. L. Roukes, and J. E. Sader, Phys. Rev. Lett. **112**, 015501 (2014).
[14] J. E. Sader, J. Sanelli, B. D. Hughes, J. P. Monty, and E. J. Bieske, Rev. Sci. Instrum. **82**, 095104 (2011).
[15] J. W. M. Chon, P. Mulvaney, and J. E. Sader, J. Appl. Phys. **87**, 3978 (2000).
[16] A. V. Oppenheim, *Discrete-Time Signal Processing* (Prentice-Hall, Upper Saddle River, NJ, 1999).
[17] J. E. Sader, B. D. Hughes, J. A. Sanelli, and E. J. Bieske, Rev. Sci. Instrum. **83**, 055106 (2012).
[18] See supplementary material at http://dx.doi.org/10.1063/1.4864086 for Mathematica notebook containing exact formulas for arbitrary β and Q_0.